Journal of Molecular Liquids 335 (2021) 116410

Contents lists available at ScienceDirect

Journal of Molecular Liquids

journal homepage: www.elsevier.com/locate/molliq

Lubricant properties of trimethylolpropane trioleate biodegradable oil: High pressure density and viscosity, film thickness, Stribeck curves and influence of nanoadditives

María J.G. Guimarey [a,b], David E.P. Gonçalves [c], José M. Liñeira del Río [a], María J.P. Comuñas [a,*], Josefa Fernández [a], Jorge H.O. Seabra [d]

[a] Laboratory of Thermophysical and Tribological Properties, NaFoMat Group, Department of Applied Physics, Faculty of Physics, University of Santiago de Compostela, 15782 Santiago de Compostela, Spain
[b] Department of Design and Engineering, Faculty of Science & Technology, Bournemouth University, Talbot Campus, Poole BH12 5BB, United Kingdom
[c] INEGI, Universidade do Porto, Faculdade de Engenharia, Rua Dr. Roberto Frias s/n, 4200-465 Porto, Portugal
[d] FEUP, Universidade do Porto, Rua Dr. Roberto Frias s/n, 4200-465 Porto, Portugal

ARTICLE INFO

Article history:
Received 19 February 2021
Revised 29 April 2021
Accepted 3 May 2021
Available online 21 May 2021

Keywords:
Viscosity-pressure coefficient
Film thickness
Friction
Trimethylolpropane trioleate
Nanoparticles

ABSTRACT

Lubricant properties of trimethylolpropane trioleate synthetic base oil (TMPTO) were experimentally determined under different temperatures, pressures and rolling-sliding conditions. With the aim to obtain the viscosity-pressure coefficient, density and viscosity measurements were performed up to 150 MPa with a falling-body viscometer and a vibrating tube densimeter, respectively. Film thickness and friction properties were determined with a ball-on-disc apparatus from temperatures of 303.15 to 353.15 K, from slide-roll ratios from 5 to 50% at 50 N (applied load). Finally, it has also been evaluated if the use of nanoparticles as additives could involve changes on film thickness and Stribeck curves of TMPTO base oil. For this aim, hexagonal-boron nitride nanoparticles (*h*-BN) and graphene nanoplatelets (GnPs) were used at mass concentrations of 0.25, 0.5 and 1.0 wt%. The viscosity of TMPTO increases from 15 mPa s (at 10 MPa and 353.15 K) to 525 mPa s (at 150 MPa and 303.15 K). The Stribeck curves for TMPTO are placed between elastohydrodynamic and mixed lubrication. All nanolubricants show very similar Stribeck curves, being the lowest friction coefficient obtained for 0.25 wt% of GnP. It has been found that for most of the experimental conditions the addition of the GnP promotes an increase of the film thickness.

1. Introduction

Environmental impact and pollution have become increasingly important as public issues. In lubrication one of the concerns is oil leakages in environment. For this reason, the formulation of new eco-friendly lubricants is an active research area. Modern esters, as trimethylolpropane triesters, are synthetic lubricant base oils alternative to mineral oils, polyalphaolefins and diesters. Trimethylolpropane trioleate (TMPTO) is being utilised as a high performance base fluid in industry [1] (hydraulic fluids, two-stroke engine oils and metalworking fluids). Recent studies [2,3] show that the TMPTO exhibits high viscosity index, excellent low temperature properties and lubricity. In addition, TMPTO is an environmental friendly fluid that has attractive anti-wear properties [2]. Therefore, it can be utilised as potential lubricating base oil. For this aim, the knowledge of its thermophysical and tribological properties is of great interest.

As far as we know, scarce studies are available on thermophysical characterization of trimethylolpropane trioleate. Qiao et al. [2] and Wu et al. [1,3] reported kinematic viscosity at 313.15 K and 373.15 K, viscosity index and pour point at atmospheric pressure, among other physicochemical properties. Zulfattah et al. [4] published density at 288.15 K and also kinematic viscosity at 313.15 K and 373.15 K at atmospheric pressure together with flash point. He et al. [5] reported density and viscosity of several ester base oils (TMPTO among others) at 0.1 MPa and 303, 348 and 398 K. In our previous works [6,7] precise density, speed of sound and dynamic viscosity (η) of TMPTO were reported from 278.15 to 373.15 K at 0.1 MPa. The viscosity and density pressure dependence under isothermal conditions and the viscosity-pressure coefficient show a lack of experimental values. In this sense, it should

* Corresponding author.
E-mail address: mariajp.comunas@usc.es (M.J.P. Comuñas).

https://doi.org/10.1016/j.molliq.2021.116410
0167-7322/

Nomenclature

A	calibration constant of the falling body viscometer, mPa s
AAD	average absolute deviation, %
$E(T)$	second-degree polynomial
EHL	elastohydrodynamic lubrication
E^*	equivalent Young modulus of the specimens, GPa
F_N	normal force, N
h_{nl}	central film thickness of the nanolubricant, nm
h_{bf}	central film thickness of neat base oil, nm
Δh	relative increment in the film thickness, –
ML	mixed lubrication
n	refractive index, –
N	number of data
h_0	film thickness, nm
p	pressure, MPa
p_{iv}	isoviscous pressure, MPa
R_X	equivalent radius in rolling direction
R_y	equivalent radius perpendicular to the rolling direction
s	parameter of Gold's equation, GPa^{-1} mm^{-2} s
S_p	dimensionless modified Stribeck parameter, –
SRR	slide-to-roll ratio, %
t	parameter of Gold's equation, –
T	temperature, K
U	rolling speed, m s^{-1}
U_S	entrainment speed, m s^{-1}
U_{disc}	speed of the disc on the contacting surfaces at EHD2 apparatus, m s^{-1}
U_{ball}	speed of the ball on the contacting surfaces at EHD2 apparatus, m s^{-1}

Greek symbols

α	pressure-viscosity coefficient, GPa^{-1}
α^*	reciprocal asymptotic isoviscous pressure coefficient, GPa^{-1}
α_{film}	universal pressure-viscosity coefficient, GPa^{-1}
α_{Gold}	pressure-viscosity coefficient proposed by Gold, GPa^{-1}
v	kinematic viscosity at 0.1 MPa, mm^2 s
η	dynamic viscosity, mPa s
η_0	dynamic viscosity at atmospheric pressure, mPa s
k	coverage factor, –
Λ	specific film thickness, –
ρ	density, kg cm^{-3}
$\rho_{0(T)}$	density of the oil at 0.1 MPa, kg cm^{-3}
μ	friction coefficient, –
σ	composite root mean square roughness, nm
σ_{ball}	surface roughness of the ball, nm
σ_{disc}	surface roughness of the disc, nm
σ_s	standard deviation, kg m^{-3}

be noted that the influence of pressure on the viscosity is crucial to develop numerical models for film thickness and friction calculations [8]. For TMPTO only relative volumes measured by Bair and Michael [9] with a piezometer at 293.15, 323.15 and 353.15 K at pressure up to 300 MPa were reported. These authors measured dynamic viscosities at 293.15, 323.15, 353.15 and 423.15 K and from 0.1 to 350 MPa. Bair and Michael [9] also reported viscosity-pressure coefficients of TMPTO at 293.15, 323.15, 353.15 and 423.15 K. Young and Bair [10] determined experimental viscosities at 298.15 K and from 0.1 to 350 MPa together with pressure-viscosity coefficient at the same temperature. Bair [11] also reported viscosities of TMPTO at 323.15 K and 373.15 K from 0.1 to 1298 MPa. Concerning tribological characterization there is also scarce literature. Thus, Young and Bair [10] reported the central entrapment depth and the friction coefficient at room temperature for a ball-on-plate sliding contact lubricated with TMPTO. He et al. [5] have determined elastohydrodynamic film thickness and coefficients of friction of TMPTO at 303, 348 and 398 K. Finally, in previous works [6,7] we have experimentally determined the friction coefficient and wear scar for TMPTO oil, using a ball (chrome steel AISI 52100) on plate (stainless steels AISI 420) configuration tribometer (stationary ball and a moving plate).

On the other hand, new packages of additives (viscosity index-improvers, friction modifiers, pour point depressants and antioxidants, among others) are needed to enhance the effectiveness and durability of the unconventional lubricants [12]. Some authors have investigated the possibility of using ionic liquids or nanoparticles as friction and wear improvers of base oils [13–19]. Focusing our attention on TMPTO, Zhu et al. [20] used as potential additives of this base oil three phosphonium ionic liquids (ILs). On the other hand, in our previous works [6,7] hexagonal boron nitride nanoparticles or graphene nanoplatelets were also used as TMPTO additives. Thus, friction coefficient and wear were analyzed under a normal force of 2.5 N and at fixed temperature, under boundary lubrication regime. When nanoparticles are used as additives, most of the studies that have been published were performed at boundary lubrication regime [17,21].

The work reported in this manuscript is focused mainly on the mixed film (ML) and on the elastohydrodynamic (EHL) lubrication regimes where the viscous properties of the lubricants are critical. This work reports density-temperature-pressure and the viscosity-temperature–pressure relationships up to 150 MPa of TMPTO. The viscosity-pressure coefficient was calculated from the density data. Furthermore, film thickness and Stribeck curves of TMPTO under an applied load of 50 N were also measured, at temperatures of 303.15, 333.15 and 353.15 K and slide-to-roll ratios from 5 to 50%. In addition, the influence of hexagonal boron nitride nanoparticles (*h*-BN) and graphene nanoplatelets (GnPs) as TMPTO additives has also been analysed on these two last properties.

2. Experimental section

2.1. Materials

The base oil trimethylolpropane trioleate (TMPTO), CAS number 57675–44- 2, was kindly provided by Croda. The sample was characterized by infrared spectroscopy (IR) and high performance liquid chromatography (HPLC) linked with mass spectrometry. More details on its composition can be found in a previous article [7], where a sample of the same lot has been used. Iolitec has supplied the hexagonal boron nitride (*h*-BN), CAS 10043-11-5, and the graphene nanoplatelets powder GnP, CAS 1034343-98-0, with a mole fraction purity of 0.990 and 0.995, respectively. For *h*-BN the bulk density is 2.29 g cm^{-3} and the nominal diameter 70 nm. The bulk density for GnP is 2.25 g cm^{-3} and the average particle diameter 15 μm and a thickness of 11–15 nm. Nanoadditives characterization (X-ray diffraction, Raman spectroscopy, SEM micrographs, TEM images and EDX analysis) was thoroughly reported in a previous work [22].

2.2. Experimental techniques

Viscosities at high pressure for the neat base oil (TMPTO) were measured with an uncertainty of 3.5% (coverage factor k = 2) by using a falling body viscometer further described in previous articles [23–25]. Fig. 1 shows the flow diagram used for viscosity experimental determination. The reliability of the equipment has been checked in previous works [26,27].

High pressure densities of TMPTO, which are needed to experimentally determine the dynamic viscosities, were measured with a HPM Anton Paar vibrating tube densimeter from 1 MPa to 100 MPa (Fig. 1) as was detailed in previous works [28–30]. The expanded uncertainties (coverage factor k = 2) are lower than $5{\cdot}10^{-3}$ g cm^{-3} over all the temperature and pressure ranges. More details on density were published in a previous work [31].

Optical interferometry is the technique most used to obtain, inside the contact zone, and with high accuracy the film thickness. In this work, an EHD2 ultra-thin film measurement apparatus (PCS Instruments) was used to measure under a 50 N load (maximum Hertz pressure of 0.66 GPa) the central film thickness (h_0) of TMPTO. This device has been further described previously [32] and allows the measurement of film thickness up to 1000 nm with a precision of 1 nm. In Fig. 2, the flow diagram used for film thickness experimental determination is presented. The tests were developed at slide-to-roll ratio (SSR) of 5% over an entrainment speed (U_s) ramp from 2 to 0.04 m s^{-1}. Three operating temperatures were tested: 303.15, 333.15 and 353.15 K. The main physical properties of the ball and the glass disc used for h_0 determination are gathered in Table 1. The refractive index (n) of the samples under study at 298.15 K is necessary to determine the film thickness with precision. For this reason, a refractometer (Mettler Toledo RA-510 M) that works at the wavelength of the D-line of sodium (589.3 nm) was utilised. The refractive index obtained at 298.15 K for TMPTO base oil is around 1.468.

To determine the friction coefficient (μ) on the EHD2 ball-on-disc apparatus, the same ball was used but the glass disc was replaced by a carbon chrome steel disc with a 100 mm diameter. Contact pressures up to 1.11 GPa were generated with an applied load of 50 N. Tests were performed using a polished disc and two rough discs with different roughness (σ_{disc}= 100 nm and σ_{disc}= 500-nm). The physical properties of the steel discs used in tribological tests are also reported in Table 1.

The friction coefficient was measured at the same temperatures (303.15, 333.15 and 353.15 K) and entrainment speed ramp as in the aforementioned film thickness tests. In this assay, the ball speed remains constant and the disc speed varies. Friction coefficient is presented through Stribeck curves determined at two *SRR* conditions (5% and 50%). To plot these curves the dimensionless specific film thickness (Λ) definition proposed by Tallian [33] was used, which includes the film thickness (h_0), see Fig. 2.

3. Results and discussion

3.1. High pressure density

As it has been explained above, density values are needed (Fig. 1) to obtain dynamic viscosities and subsequently to obtain the pressure-viscosity coefficient. In Table 2 density experimental values are reported for TMPTO oil from 278.15 to 398.15 K and from 1 to 100 MPa. At 278.15 K the density increases around 4% with the pressure increase and at 398.15 K around 7%, over the complete pressure interval. The density decreases with temperature is around 2–3% for all the isobars. In Fig. 3 the density-pressure-temperature surface for TMPTO is plotted. In order to correlate the experimental densities of the base oil over the entire temperature and pressure ranges, the following Tait-like equation was employed [29,30]:

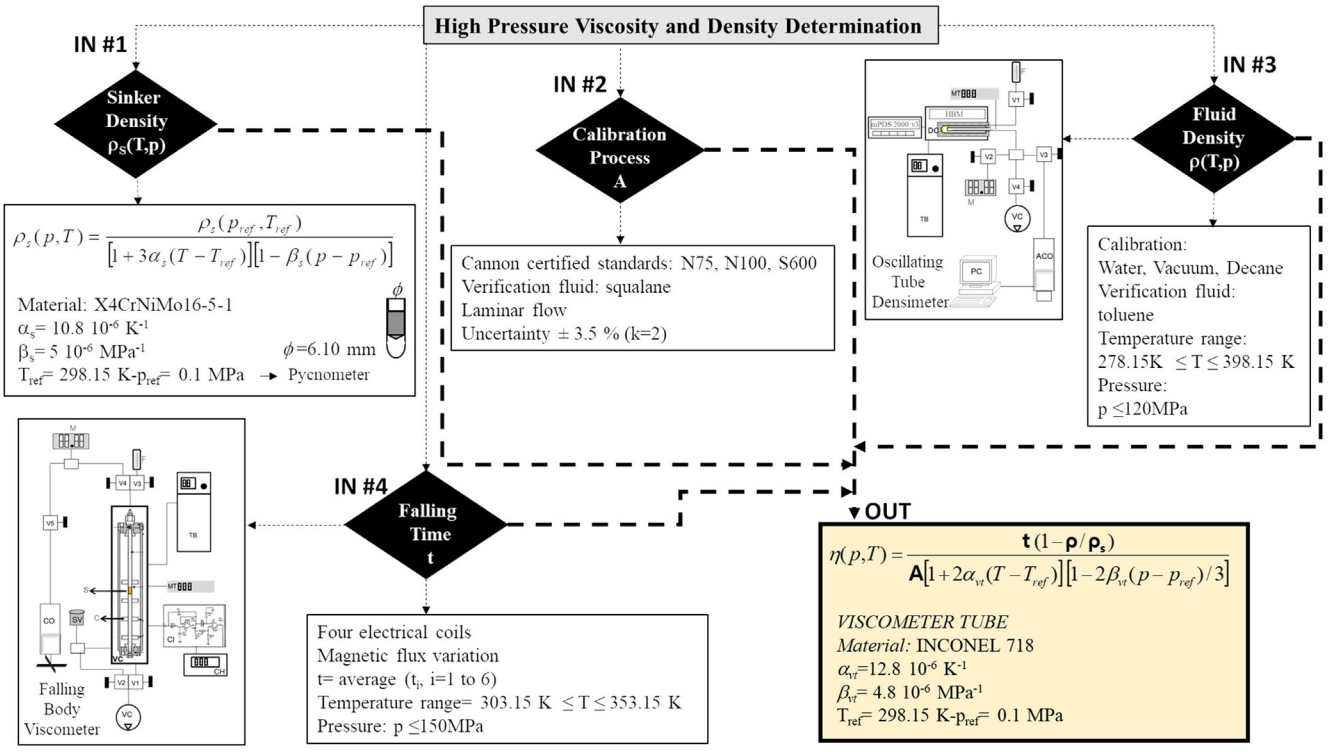

Fig. 1. Flow diagram of the procedure employed for high pressure density and viscosity experimental measurements.

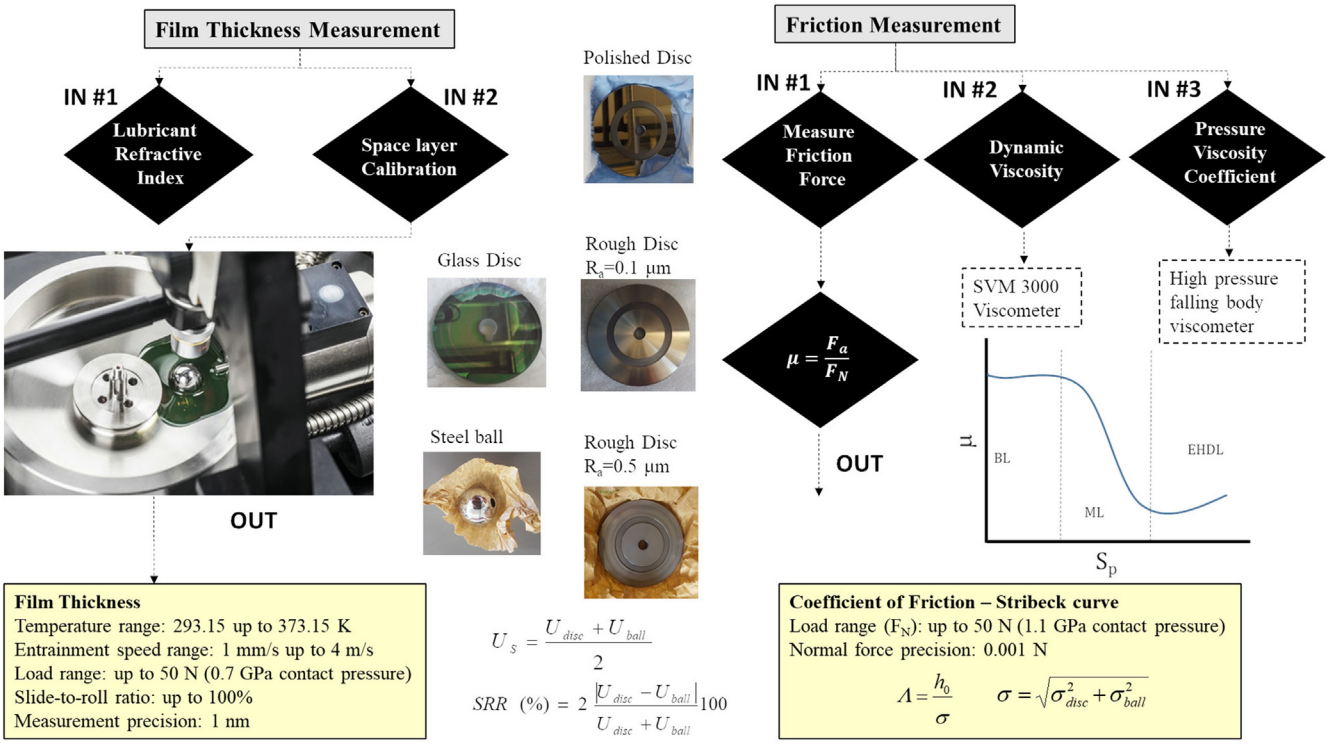

Fig. 2. Scheme of the procedure employed for film-thickness and friction coefficient experimental determination.

Table 1
Properties of the ball and the discs used in EHD2 ultra-thin film apparatus.

Property	Ball	Glass disc	Steel disc		
			Polished	Rough 1	Rough 2
Elastic modulus E/GPa	210	64	210	210	210
Poisson coefficient υ/-	0.29	0.2	0.29	0.29	0.29
Radius R/mm	19.05	50	50	50	50
Surface roughness σ/nm	20	5	20	100	500

Table 2
Density values, ρ[a], in kg cm^{-3}, for the base oil TMPTO at different temperatures, T[b], and pressures, p.[c]

T/K					
p/MPa	*278.15*	*288.15*	*293.15*	*298.15*	*313.15*
1	928.77	922.14	918.94	915.70	905.88
5	930.80	924.24	921.08	917.89	908.20
10	933.28	926.78	923.66	920.52	910.98
20	937.98	931.65	928.63	925.60	916.36
40	946.70	940.77	937.96	935.11	926.33
60	954.68	948.94	946.23	943.52	935.25
80	962.27	956.80	954.19	951.58	943.57
100	969.26	964.04	961.53	959.04	951.35
p/MPa	*333.15*	*348.15*	*353.15*	*373.15*	*398.15*
1	892.64	882.71	879.45	866.29	850.00
5	895.15	885.39	882.18	869.26	853.37
10	898.16	888.59	885.46	872.81	857.37
20	903.93	894.69	891.68	879.52	864.84
40	914.58	905.88	903.05	891.63	877.99
60	924.06	915.82	913.13	902.32	889.50
80	932.87	924.95	922.35	911.97	899.71
100	941.04	933.43	930.92	920.93	909.15

[a] Expanded density uncertainty (k = 2): 0.7 · 10^{-3} g cm^{-3} for T ≤ 373.15 K, 5·10^{-3} g cm^{-3} at 373.15 and 398.15 K and 0.1 MPa, and 3 · 10^{-3} g cm^{-3} at T ⩾ 373.15 K and p > 0.1 MPa.
[b] Expanded temperature uncertainty (k = 2): 0.02 K.
[c] Expanded pressure uncertainty (k = 2): 0.02 MPa.

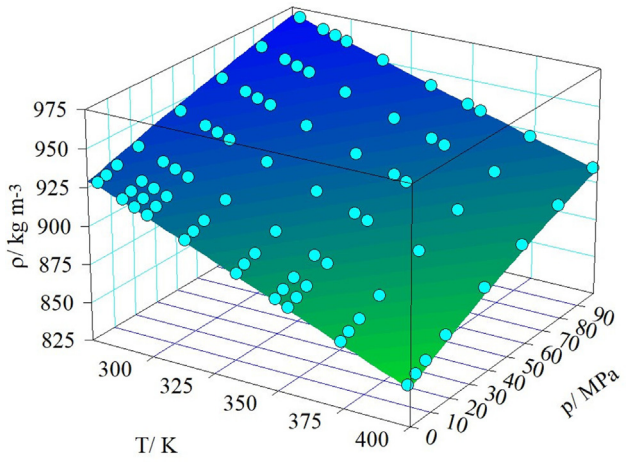

Fig. 3. Density-pressure-temperature surface for TMPTO lubricant: circles experimental data and $p\rho T$ surface obtained from Eq. (1) and parameter values of Table 3.

$$\rho(T,p) = \frac{A_0 + A_1 T + A_2 T^2}{1 - C\ln\left(\frac{B_0 + B_1 T + B_2 T^2 + p}{B_0 + B_1 T + B_2 T^2 + 0.1\ MPa}\right)} \quad (1)$$

Density values at 0.1 MPa for TMPTO needed for Eq. (1) have been taken from previous work [7]. In Table 3, where parameters and statistical deviations are reported, it can be shown as the standard deviation (σ_s) is lower than 0.9 kg m^{-3}. We have compared density values obtained from Eq. (1) with those previously reported at atmospheric pressure by Zulfattah et al. [4] at 288.15 K and by He et al. [5] at 303, 348 and 398.15 K. The average deviations obtained with these authors are 0.4% and 0.12%, respectively. The TMPTO sample studied by He et al. [5] was obtained from China Petrochemical Corporation (Sinopec). Unfortunately, these authors [5] do not report purity and other characteristics. According with the authors densities were measured from accurate mass and volume measurements; but no uncertainty of the density data was reported in their article.

In the case of Zulfattah et al. [4] the densities were measured with a SVM 3000 Stabinger viscometer, which is same model used for atmospheric pressure in our previous work [7]. Zulfattah et al. [4] have not reported the purity or lot number of their TMPTO sample. Eq. (1) has also been used to extrapolate density from 100 to 150 MPa (maximum working pressure of the high-pressure falling body viscometer). This procedure [34] does not have any significant effect on viscosities at high pressure.

3.2. High pressure viscosity

The dynamic viscosity values at high pressures for TMPTO are reported in Table 4. This transport property ranges from 15 mPa s (at 353.15 K and 10 MPa) to 521 mPa s (at 303.15 K and 150 MPa). The pressure effect on viscosity becomes smaller as temperature increases. Hence, at T = 303.15 K the viscosity at 150 MPa is around seven times higher than that at 10 MPa, and at 353.15 K four times higher. The viscosity data of TMPTO at high pressure, together with the viscosities at 0.1 MPa published in our previous work [7], were correlated using the following equation proposed by Comuñas et al. [35]:

$$\eta(p,T) = A\exp\left(\frac{B}{T-C}\right)\left(\frac{p + E_0 + E_1 T + E_2 T^2}{0.1\ MPa + E_0 + E_1 T + E_2 T^2}\right)^D \quad (2)$$

where the values of the parameters A, B and C were obtained by fitting viscosity data at atmospheric pressure as a function of temperature. The parameter D, as well as E_0, E_1 and E_2, were obtained by curve fitting of the experimental viscosities at high pressures. Table 5 reports the results obtained for the viscosity correlation by using Eq. (2). This equation leads to a good correlation of the experimental values with AADs around 1%. Fig. 4 shows the experimental viscosity data of TMPTO lubricant as function of pressure and the correlation obtained with (Eq. (2)), over each isotherm. Comparisons have been performed between the viscosity values obtained in this work and those previously reported by other authors. Thus, average relative deviation between the data obtained from Eq. (2) and the values reported by He et al. [5] at 303 and 348 K is 6.3%. When compared to the viscosities of Qiao et al. [2] at 313.15 K and 373.15 K, an absolute average deviation of 4.9% is obtained. At the same temperatures, AAD of 3% and 2% are obtained when compared to the results of Wu et al. [1,3] and with Zulfattah et al. [4], respectively. Note that the TMPTO sample used by Wu et al. [1,3] was synthesized from trimethylolpropane (TMP) using a esterification process. In the case of Qiao et al. [2], TMPTO was synthesized through dehydration condensation from oleic acid (OA) and trimethylolpropane (TMP). These authors [1–3] have not reported the purity of their TMPTO samples.

The comparisons with the data reported by Bair [11], Bair and Michael [9] and Young and Bair [10] have been performed avoiding extrapolations, i.e. at the operating temperatures (278.15–353.15 K) and pressures (0.1–150 MPa) of Eq. (2). AADs of 1.4% and 0.7%, as well as maximum deviations of 4.0% and 1.1%, were obtained with the values measured by Bair and Michael [9] and Bair [11] respectively. Comparing with Young and Bair [10] viscosities at 298.15 K, the relative deviations range from 1.3% (at 0.1 MPa) to 9.9% (at 150 MPa) both. In this sense, we must point out that in our work the dynamic viscosity was measured at high pressures from 303.15 K to 353.15 K. Hence, in the database used to fit the experimental data to Eq. (2), there is only the dynamic viscosity value at 298.15 K and 0.1 MPa [7] and no value for higher pressures at this temperature. Bair and Michael [9] studied a TMPTO base stock produced through transesterification of a vegetable oil derived triglyceride. No information has been provided on TMPTO samples in the above articles [9–11].

The dynamic viscosity of trimethylolpropane trioleate was also compared with that previously reported for other polyol esters (neopentylglycol esters, trimethylolpropane esters, pentaerythritol esters and dipentaerythritol esters). Fig. 5 shows the dynamic viscosity at 313.15 K and at 0.1 and 50 MPa (when available). For the polyol esters, having the same ester groups number, viscosity increases with the length or with the branching degree of the alkyl chain. Viscosity of polyol esters increases with the ester groups number. Similar relative viscosity increases are obtained, when the pressure grows, for trimethylolpropane esters, pentaerythritol esters and dipentaerythritol esters. Thus, the viscosity at 50 MPa is around twice higher than that obtained at 0.1 MPa, for each one of these polyesters.

Table 3
Correlation results for TMPTO oil density (Eq. (1)).

Parameters	
A_0/kg m^{-3}	1102.69
A_1/kg m^{-3} K^{-1}	−0.62106
$10^5 \cdot A_2$/kg m^{-3} K^{-2}	−4.6575
$10^2 \cdot C$	6.84581
B_0/MPa	291.196
B_1/MPa K^{-1}	−0.82926
$10^3 \cdot B_2$/MPa K^{-2}	0.629121
σ_s/kg m^{-3}	0.9
AAD/%	0.1
Bias/%	0.3
MD/%	−0.07

Table 4
Dynamic viscosity values, η/mPa s, for the base oil (TMPTO) as a function of the temperatures, *T*, and pressures, *p*.

p/MPa	*T*/K					
	303.15	313.15	323.15	333.15	343.15	353.15
10	79.50	51.85	34.65	24.93	19.78	15.06
15	86.56	56.38	37.73	26.94	21.02	15.96
25	101.9	66.10	44.29	31.23	23.71	17.90
50	148.1	94.77	63.36	43.83	31.70	23.64
75	208.4	131.0	86.96	59.65	41.93	30.95
100	287.3	176.8	116.2	79.48	55.01	40.28
125	390.3	234.7	152.3	104.4	71.76	52.17
150	525.0	307.8	197.0	135.6	93.20	67.34

Expanded uncertainties (k = 2) are $U(T)$ = ±0.1 K, $U(p)$ = ±0.2 MPa and $U_r(\eta)$ = 3.5%.

Table 5
Obtained parameters for Eq. (2).

Parameters	Values
A/m Pa s	0.08146
B/K	1045.3
C/K	147.83
D	4.6038
E_0/MPa	−192.8
E_1/MPa K^{-1}	1.3308
10^3 E_2/MPa K^{-2}	0.68715
AAD/%	1.0
Bias/%	−0.3
MaxD/%	5.3

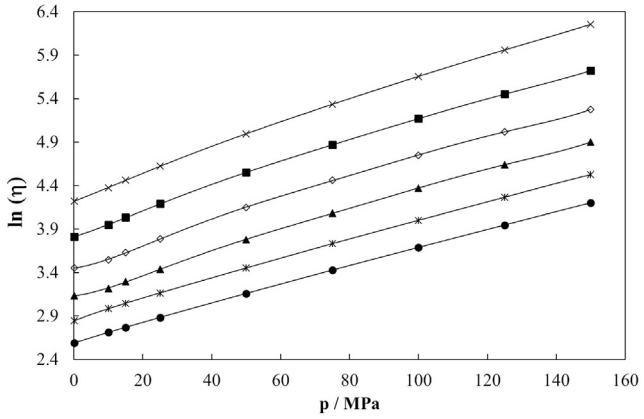

Fig. 4. Dynamic viscosity, η, for TMPTO. (●) T = 353.15 K, (⁎) T = 343.15 K, (▲) T = 333.15 K, (◇) T = 323.15 K, (■) T = 313.15 K and (×) T = 303.15 K. Solid lines are the results obtained from correlation with Eq. (2).

3.3. Pressure-viscosity coefficient

The pressure-viscosity coefficient (α) is another relevant property in EHL lubrication. This coefficient is difficult to determine experimentally, being the subject of controversy in the literature. According to Bair and other researchers [19,40] this parameter should be experimentally determined performing viscosity measurements at high pressure, by using a high-pressure viscometer. Contrarily, Spikes and other researchers [41,42] determine the pressure viscosity from film measurements. In addition, α can be estimated using empirical prediction equations in order to determine the film thickness. In this work, α values for the base oil (TMPTO) were determined using high pressure–viscosity measurements (α*and α_{film}) and Gold et al. [43] predictive method (α_{Gold}).

Firstly, the pressure-viscosity coefficient was obtained from the experimental viscosity-pressure-temperature correlation (Eq. (2)) and the procedure proposed by Bair et al. [44] for the universal pressure-viscosity coefficient (α_{film}) as in previous works [26,27]. The values obtained for α_{film} and α^* as function of temperature for TMPTO lubricant are presented in Table 6. α_{film} values of 12.5 GPa^{-1} and 10.7 GPa^{-1} were obtained at 323.15 K and 353.15 K, respectively. These values are in agreement with previously published data (12.8 GPa^{-1} and 11.0 GPa^{-1}) by Bair and Michael [9] at the same temperatures. Young and Bair [10] have also published the pressure-viscosity coefficient but at 298.15 K (13.1 GPa^{-1}). This temperature is outside the experimental temperature interval (303.15 K to 353.15 K) of the viscosity-pressure measurements. We have also compared the α_{film} obtained in this work at 303.15 K with that published by He et al. [5] at 303 K, obtaining relative deviations around 6.6%. This is an excellent result taking into account that our value is obtained from viscosity measurements at high pressure and that of He et al. [5] from measured film thickness and the Yokoyama-Spikes equation by using diisooctyl phthalate (DIOP) as reference fluid. In Fig. 6 the universal pressure-viscosity coefficient (α_{film}) is plotted for several polyol esters. Pentaerythritol tetraoleate (PETO) and pentaerythritol tetra-2-ethylhexanoate (PEB8) show the highest α_{film} values. At 303.15 K, TMPTO has universal pressure-viscosity coefficients close to those of pentaerythritol esters (PEC5, PEC7 and PEC9), but its viscosity is much higher as Fig. 5 shows. This fact would lead to a remarkable effect in the film thickness, and subsequently different tribological behaviours.

The pressure–viscosity coefficient for TMPTO was also estimated from the following equation proposed by Gold et al. [43] that relates this coefficient with the kinematic viscosity, ν, at 0.1 MPa:

$$\alpha_{Gold} = s\nu^t \tag{3}$$

Gold et al. [43] have used a database of 28 lubricants including mineral, synthetic and vegetable oils to determine *s* and *t* values for six lubricant types. The α_{Gold} of TMPTO base oil was estimated by using the two parameters (*s*, *t*) values reported by these authors [43] for biodegradable esters (*s* = 6.605 and *t* = 0.136). These parameters are valid from 278.15 to 353.15 K. The kinematic viscosity for TMPTO need in Eq. (3) was also taken from our previous work [7]. As it is presented in Table 6 the pressure-viscosity coefficients obtained from both the procedure proposed by Bair et al. [44] (α_{film}) and Eq. (3) (α_{Gold}) decrease with the temperature rise. It is found that over all the temperature interval, α_{film} values are higher than the α_{Gold} values. We have found deviations around 16% at 303.15 K, 13% at 333.15 K and 10% at 353.15 K between α_{film} and α_{Gold} values.

3.4. Central film thickness

Table 7 reports the central film thickness (h_0) experimental values at the different temperatures and speeds for TMPTO. As shows Fig. 7, the film thickness decreases remarkably when the temperature rises and increases when the entrainment speed grows. Similar behaviour has been observed by He et al. [5] by using a PCS EHD instrument under a load of 20 N and at 303, 348 and 398 K. These authors did not publish the numerical values of h_0, presenting the results as plots.

The film thickness can also be obtained theoretically from the following equation proposed by Hamrock and Dowson [46]:

$$h_0 = 2.69R_X\left(\frac{\eta_0 U_S}{E^* R_X}\right)^{0.67}(\alpha E^*)^{0.53}\left(\frac{F_N}{E^* R_X^2}\right)^{-0.067}\left[1-0.61e^{\left(-0.73\left(1.03\frac{R_Y}{R_X}^{0.64}\right)\right)}\right] \tag{4}$$

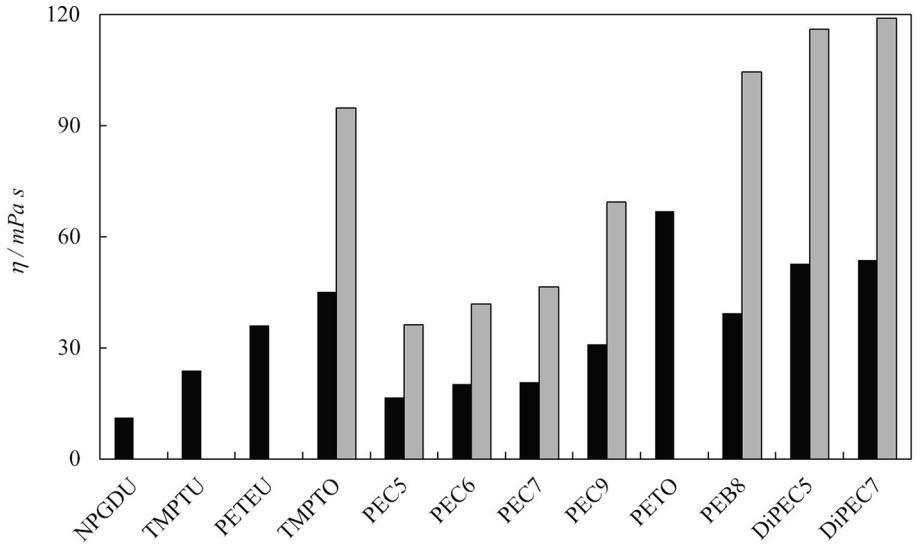

Fig. 5. Dynamic viscosity of several polyol esters at 313.15 K and at (■) 0.1 MPa or (▒) 50 MPa: neopentylgycol diundecenoate (NPGDU) [36], trimethylolpropane triundecenoate (TMPTU) [36], trimethylolpropane trioleate (TMPTO) ([7] at 0.1 MPa and this work at 50 MPa), pentaerythritol tetraoleate (PETO) [5], pentaerythritol tetrahexanoate (PEC6) [11], pentaerythritol tetrapentanoate (PEC5) and pentaerythritol tetraheptanoate (PEC7) [37], pentaerythritol tetraundecenoate (PETEU) [36], pentaerythritol tetra-2-ethylhexanoate (PEB8) and pentaerythritol tetranonanoate (PEC9) [38], dipentaerythritol tetrapentanoate (DiPEC5) and dipentaerythritol tetraheptanoate (DiPEC7) [39].

Table 6
Pressure–viscosity coefficients determined by using Bair equation (α_{film} and α^*) and Gold equation (α_{Gold}) for TMPTO.

T/K	α_{film}/GPa^{-1}	α^*/GPa^{-1}	α_{Gold}/GPa^{-1}
303.15	14.1	13.2	11.9
313.15	13.3	12.4	11.2
323.15	12.5	11.7	10.7
333.15	11.8	11.1	10.3
343.15	11.2	10.5	9.9
353.15	10.7	10.0	9.6

being R_X is the equivalent radius in rolling direction, η_0 is the dynamic viscosity at test temperature and atmospheric pressure, E^* is the equivalent Young modulus of the specimens, U_S is the entrainment speed, α is the pressure–viscosity coefficient at the test temperature, F_N is the normal load and R_y is the equivalent radius perpendicular to the rolling direction.

The film thickness experimentally determined for TMPTO base oil by optical interferometry has been compared with the h_0 values obtained from Eq. (4) using α_{film}, α^* and also the pressure-viscosity coefficient due to Gold et al. (α_{Gold}). The absolute average deviations (AADs%) between measured film thickness and estimated film thickness were 11.3% (303.15 K), 2.5% (333.15 K) and 2.9% (353.15 K) if α_{film} is used, 7.1% (303.15 K), 3.1% (333.15 K) and 7.0% (353.15 K) for α^* and 2.7% (303.15 K), 6.7% (333.15 K), and 9.2% (353.15 K) from α_{Gold} values. It is observed that at 303.15 K the experimental film thickness is closer to the h_0 calculated with the Gold et al. equation. When the temperature rises, more agreement is found with the film thickness determined from the experimental high-pressure viscosities (α_{film} and α^*). In Fig. 8, it can be observed that the use of α_{Gold} to calculate the film thickness leads to an underestimation of h_0 at 333.15 K and 353.15 K.

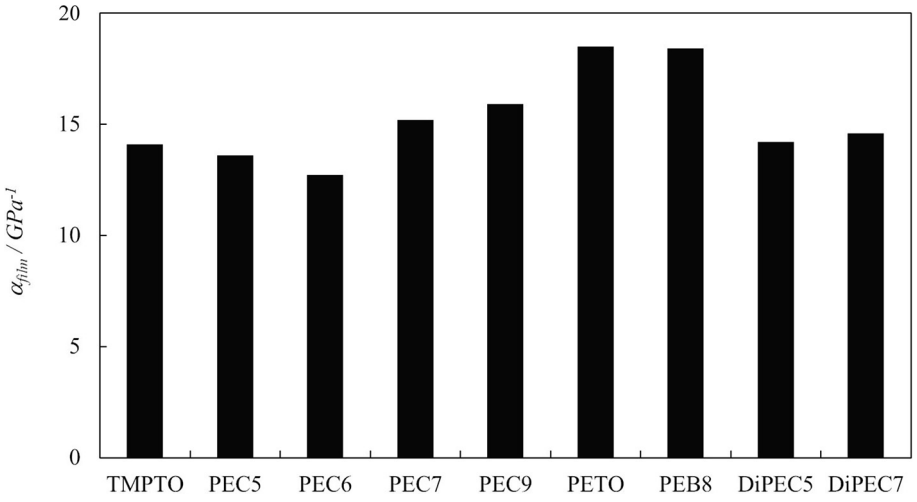

Fig. 6. Pressure-viscosity coefficient (α_{film}) at 303.15 K for several base oils: TMPTO [this work], PEC5, PEC7, PEB8, PEC9, DiPEC5 and DiPEC7 [45]. For pentaerythritol tetrahexanoate (PEC6) the α_{film} value is at 313.15 K [11] and for pentaerythritol tetraoleate (PETO) [5] is the reciprocal asymptotic isoviscous obtained from film thickness at 303 K.

Table 7
Experimental central film thickness, h_0/nm, for TMPTO oil at different entrainment speeds, U_s/m s^{-1}, and temperatures.

U_s/m s^{-1}	303.15 K	313.15 K	323.15 K	U_s/m s^{-1}	303.15 K	313.15 K	323.15 K
2.00	427	204	144	0.24	110	51	35
1.40	348	162	119	0.12	67	31	20
0.99	274	137	93	0.08	52	25	17
0.69	214	107	72	0.06	40	21	13
0.49	166	84	57	0.04	31	18	12

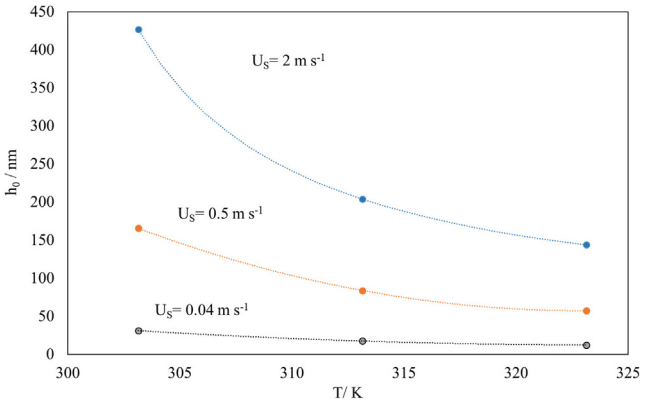

Fig. 7. Central film thickness for neat TMPTO at SRR = 5%: (•) experimental measurements; (·····) polynomial fitting for guided-eye.

3.5. Stribeck curves

The Stribeck curves (coefficient of friction, μ, versus specific film thickness, Λ) of TMPTO were determined from traction force measurements. Λ is defined as the ratio of the central film thickness (h_0) to composite root mean square roughness (σ), see Fig. 2. The values of h_0 were taken from the experimental measurements (Table 7) and σ is obtained as the root mean square of the roughness of each specimen (Fig. 2). In the earlier studies [47–49] on lubrication regimes it has been concluded that when $\Lambda > 3$ the oil film is thick enough to ensure there is no asperity contact between the surfaces and the system is under full-film lubrication (being for $\Lambda > 5$ hydrodynamic lubrication and for $3 < \Lambda < 5$ EHL lubrication). Boundary lubrication is expected when $\Lambda < 1$ being the lubricating film not thick enough to prevent contact between the surfaces, the mixed regime is observed for moderate film thicknesses ($1 < \Lambda < 3$). Subsequently, Spikes and Guangteng [50] concluded that the mixed lubrication regime appears at a different lambda range, ($0.1 < \Lambda < 2$). Lately, Spikes and Olver [51] reviewed later findings on mixed film lubrication and concluded that this regime expands in the range of $0.05 < \Lambda < 3$, therefore the boundary film lubrication takes place for $\Lambda < 0.05$. More recently, Zhu and Wang [52] concluded that if boundary lubrication is defined when more than 90% of load supported by the asperity contact, its corresponding Λ value is generally smaller than 0.01–0.05, being the maximum Λ values for mixed range between 1.0 and 1.5. Fig. 9 shows that the obtained Stribeck curves for TMPTO for 5% and 50% SRR are placed from EHL to boundary lubrication. Comparing Fig. 9a and b, an increase in the friction coefficients can be observed when the SRR increases. This is expected, since for a constant entrainment speed, if the SRR increases, therefore the sliding speed is higher, leading to an increase in the coefficient of friction [53]. In addition, Fig. 9 seems to indicate that boundary regime appears at Λ values lower than 0.1–0.15 for 5% SRR and lower than 0.05 for 50% SRR.

On the other hand, the effects of the roughness and temperature are analysed, keeping constant the remaining operating conditions (SRR 5% and F_N = 50 N). The friction coefficient (μ) increases as the disc roughness as well as the temperature rise, except in polished disc conditions (high Λ values) where the friction coefficient is lower at 353.15 K and 333.15 K than at 303.15 K. With increasing temperature, the Stribeck curve shifts towards smaller Λ values due to h_0 decreases (Fig. 8). For instance, for the roughness of 100 nm and for U = 2 m s^{-1}, the parameter decreases from Λ around 3.9 at 303.15 K to Λ around 1.3 at 353.15 K. Analysing the Fig. 9, it can be observed that when the discs are changed, increasing the roughness from 20 nm to 500 nm, the Λ values become smaller. As an example, for the temperature of 303.15 K and for U = 2 m s^{-1}, Λ decreases from 14.2 (polished disc, 20 nm) to 0.8 (rough disc, 500 nm).

Theoretically a single curve should describe the friction behaviour along the whole lubrication range. However, such perfect match is not clearly observed. In fact, while the film thickness (h_0) takes into account the materials properties (disc and lubricant), the kinematic and load conditions and the contact geometry; the roughness parameter used (σ) only takes into account the average of the peaks and valleys' heights which might be insufficient. In summary, a more complex description of the surface roughness is necessary to reach such perfect match, which is a topic under research.

3.6. Influence of nanoadditives

With the aim of evaluating if the use of nanoadditives could promote any changes on the film thickness and Stribeck curves of the base oil, hexagonal boron nitride nanoparticles (*h*-BN) and graphene nanoplatelets (GnPs) were used as additives of trimethylolpropane trioleate (TMPTO). An ultrasonic stirrer was used to disperse the nanoparticles in TMPTO. In the case of *h*-BN, a UP200S probe sonicator (Hielscher) coupled with a 14 mm (diameter) tip was used. The sonication conditions were 93.75 μm of amplitude (which means 75% of the probe sonicator power) for 4 h in pulse mode. To avoid overheating, the samples were also submerged in an ice-water bath. GnPs were dispersed during 6 h into TMPTO by means of ultrasonic bath (model 3000513, Ultrasons, JP Selecta S.A.) operating at a generator power of 150 W and a sonication frequency of 42 kHz. A high-quality precision balance Mettler Toledo PR1203 with a readability of 0.00001 g was used to determine the nanoparticles mass concentration. Thus, six nanolubricants at mass concentrations of 0.25, 0.50, and 1.0 wt% for *h*-BN and GnP, respectively, were prepared. Visual control has been used to ensure that nanolubricants have a temporal stability longer than the time needed to perform the film thickness and friction tests. In this sense, we must take into account that in previous works [6,7] temporal stabilities higher than 90 h and 24 h were observed for TMPTO + GnP and TMPTO + *h*-BN, respectively. Over these time intervals, no clear precipitation was observed at the bottom or on the walls the vials, neither any sign of stratification (colour change) was observed for all the nanolubricant samples.

The film thickness of the nanolubricants (h_{nl}) has been measured at the same conditions as the neat oil TMPTO. As has been detailed above, the refractive index (n) of the samples under study is necessary to determine the film thickness with precision. For this

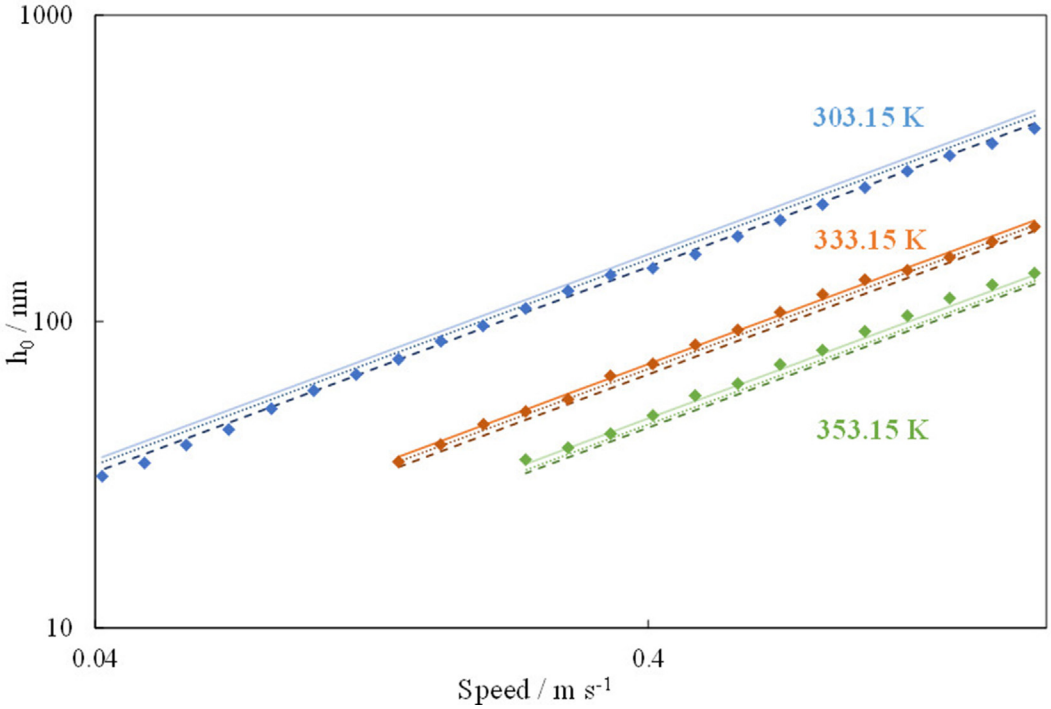

Fig. 8. Central film thickness for neat TMPTO at SRR = 5%: (◆) experimental measurements; calculated from Hamrock and Dowson equation using: (—) pressure-viscosity coefficient (α_{film}), (····) reciprocal asymptotic isoviscous pressure coefficient (α^*) and (– –) the pressure-viscosity coefficient obtained from the Golds equation (α_{Gold}).

reason, the refractive index of nanolubricants was measured at 298.15 K obtaining values (1.468–1.469) similar to that obtained for TMPTO (1.468). Consequently, the same refractive index value was used for TMPTO and the nanolubricants. We have determined at each entrainment speed the relative increments (Δh) between the film thickness of each nanolubricant and the film thickness of the TMPTO neat base oil, as follows:

$$\Delta h = \frac{h_{nl} - h_{bl}}{h_{bl}} \tag{5}$$

being h_{nl} and h_{bl} the nanolubricant and the TMPTO neat oil film thickness, respectively. Thus, when $\Delta h > 0$, the film thickness of the nanolubricant is higher than the film thickness of the neat base oil, the opposite for $\Delta h < 0$. In Fig. 10, we have plotted for each nanolubricant the number of experimental data that present $\Delta h > 0$ or $\Delta h < 0$ for different nanoparticle mass concentrations and different temperatures.

It should be noted that the addition of GnP leads to an increase in the film thickness for the most of the entrainment speeds, temperatures and mass concentrations. Thus, with GnP only a significant number of points is found with $\Delta h < 0$ at 353.15 K and 1 wt %. Nevertheless, the film thickness for nanolubricants containing *h*-BN nanoparticles, is lower than that of the neat oil (TMPTO) in many experimental conditions. It should also be noted that a thicker lubricant film ($\Delta h > 0$) will provide and increased protection of the surfaces. The maximum increase in the film thickness was observed, at 0.07 m s^{-1} and at 303.15 K, for TMPTO/0.25 wt% GnP nanolubricant for which the increase in h_0 is around 14% with respect to neat TMPTO. This result agrees with that obtained in [7], for the viscous behaviour of nanolubricants containing GnP and *h*-BN nanoadditives. Thus, it was observed [7] that generally, for the same mass concentration, the effect of the GnP on the viscosity is much higher than that of *h*-BN, which is important since this is the main lubricant property affecting the film thickness together with the pressure-viscosity coefficient. Nevertheless, for both GnP and *h*-BN nanoparticles a regular dependence of the film thickness with the mass concentration of nanoparticles is not observed. This last fact is also usual for other tribological properties as wear and friction coefficient [54].

The Stribeck curves for all nanolubricants were measured at the same conditions as those previously detailed for the neat base oil (TMPTO) being those for the three discs (σ_{disc} = 500 nm; σ_{disc} = 100-nm and polished disc) and the different operating conditions very similar. As an example, the friction coefficient values (μ) of the base oil and the nanolubricants at 303.15 K versus lambda (Λ) are shown in Fig. 11. For the nanolubricant containing 0.25 wt% of GnP we obtain the lowest friction coefficient with respect to the neat base oil. This result is in agreement with those obtained for film thickness. For a fixed speed of 2 m s^{-1} and a temperature of 303.15 K (conditions for maximum increase of film thickness), friction reductions of 1.2, 8.4 and 8.7% were obtained for the polished disc and the rough discs (σ_{disc} = 100 nm and σ_{disc} = 500 nm, respectively) lubricated with TMPTO/0.25 wt% GnP. Liñeira del Río et al. [7] have also investigated the tribological behaviour of nanolubricants composed by the TMPTO oil containing 0.05, 0.10, 0.25 and 0.50 wt% of GnP under other operating conditions. These authors have used a CSM Standard tribometer operating in reciprocating mode with a ball on plate geometry. These tests were conducted under a working load of 2.5 N (maximum contact pressure of 0.88 GPa) and a maximum speed of 0.10 m s^{-1} at room temperature. These authors have also obtained the best combined antifriction-antiwear performance for the nanolubricant with 0.25 wt% of GnP.

4. Conclusions

The lubricant properties (high pressure viscosity and density), film thickness and Stribeck curves) were investigated for a biodegradable synthetic base oil: trimethylolpropane trioleate. The following features were achieved:

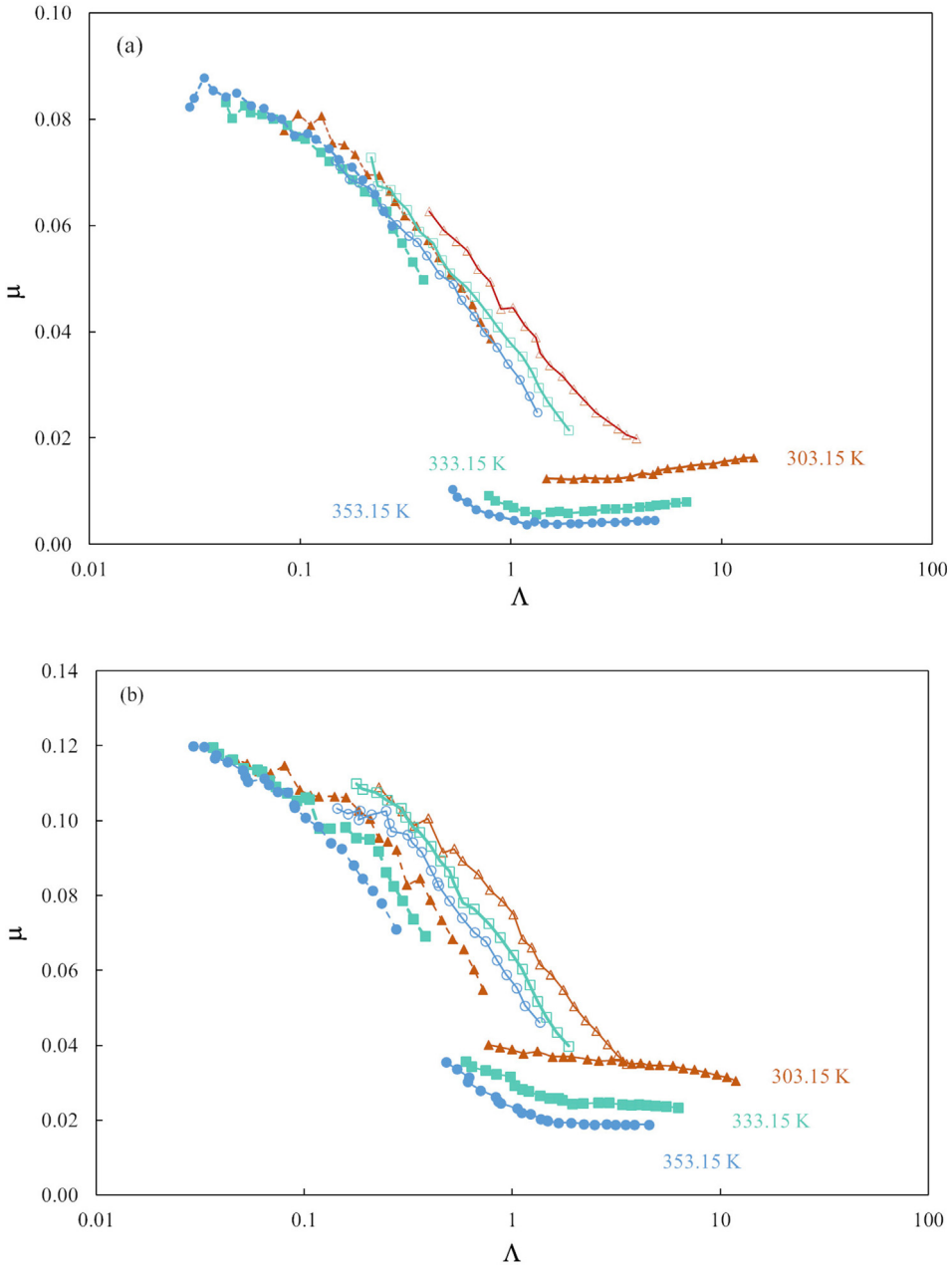

Fig. 9. Stribeck curves of the TMPTO base oil for rough and polished discs at three temperatures: (a) 5% SRR and (b) 50% SRR.

- Two correlation equations are reported to obtain densities and viscosities of TMPTO over the interval (278.15–398.15 K and 0.1–100 MPa) and (278.15–353.15 K and 0.1–150 MPa), respectively.
- The viscous behaviour of TMPTO was compared with that of other polyol esters finding that the viscosity increases with the length or the branching degree of the alkyl chains and with the number of ester groups.
- Deviation around 11% (at 303.15 K) and around 3% (at 353.15 K) were observed between the film thickness experimentally determined by optical interferometry, and that obtained from Hamrock and Dowson equation (using high pressure viscosity data).
- Gold et al. equation for ester lubricants underestimates the viscosity-pressure coefficient, and consequently the film thickness.
- For most of the entrainment speeds, temperatures and mass concentrations, the addition of the graphene nanoplatelets promotes a rise of the film thickness. This is not the case of boron hexagonal nitride nanoparticles for which a reduction in the film thickness was observed in different experimental conditions. A maximum increase in the film thickness of 14% was observed at 0.07 m s^{-1} and at 303.15 K, for TMPTO/0.25 wt% GnP nanolubricant in comparison with neat TMPTO.
- The friction coefficient of nanolubricants is very similar to those of TMPTO neat oil, thus slightly lower values are obtained for TMPTO/0.25 wt% GnP under a SRR of 5% at all temperatures. For instance, for the lowest temperature (303.15 K) the highest reduction was around 13% at 0.169 m s^{-1} and σ_{disc} = 500 nm.

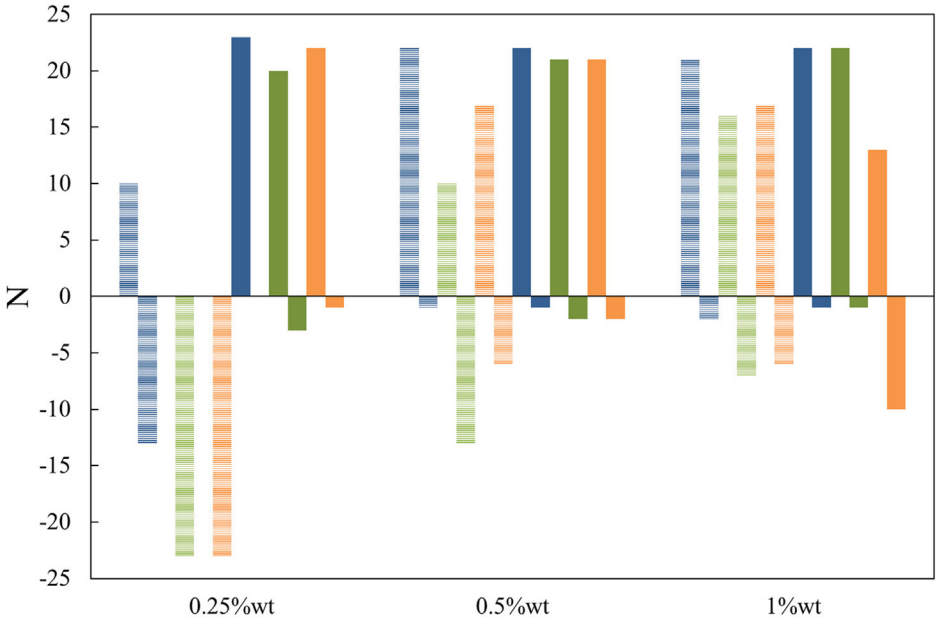

Fig. 10. Number of experimental data (N), overall the entrainment speed range, with positive or negative Δh value as a function of the nanoparticle mass concentration and at 303.15 K (blue), 333.15 K (green) and 353.15 K (orange): GnP (■) and *h*-BN (▤).

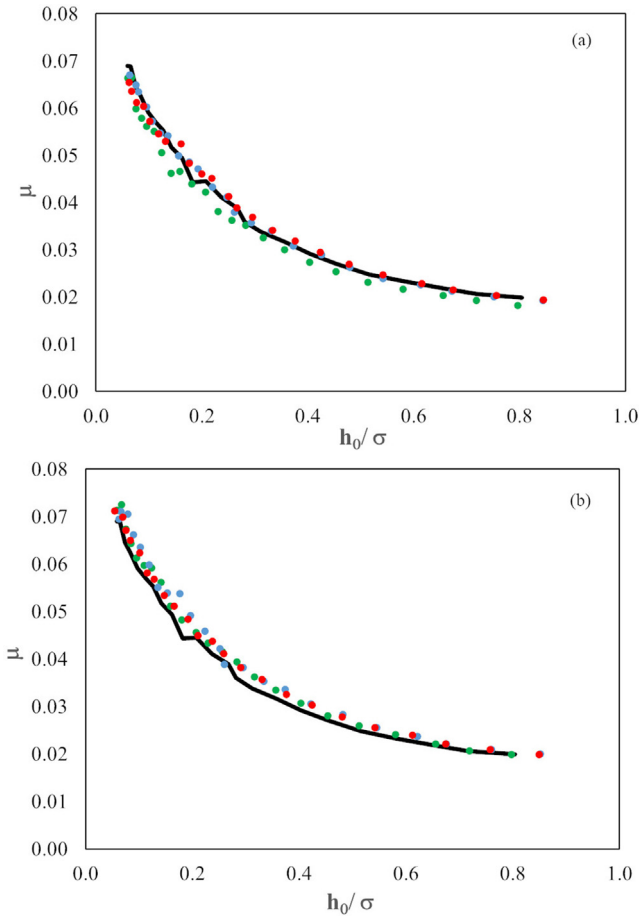

Fig. 11. Effect of the use of nanoparticles on the Stribeck curves of TMPTO at 303.15 K (F_N = 50 N, SRR5% and σ_{disc} = 100 nm) for (a) TMPTO + GnP and (b) and TMPTO + BN: (●) 1 wt%, (●) 0.5 wt%, (●) 0.25 wt% and (▪) 0 wt% (neat TMPTO).

CRediT authorship contribution statement

María J.G. Guimarey: Writing - original draft, Investigation. **David E.P. Gonçalves:** Investigation, Visualization. **José M. Liñeira del Río:** Investigation, Validation. **María J.P. Comuñas:** Methodology, Writing - review & editing. **Josefa Fernández:** Supervision, Conceptualization. **Jorge H.O. Seabra:** Supervision.

Declaration of Competing Interest

The authors declare that they have no known competing financial interests or personal relationships that could have appeared to influence the work reported in this paper.

Acknowledgments

Authors acknowledge Croda for the TMPTO lubricant provided. Spanish Ministry of Economy and Competitiveness, the European Regional Development Fund programme and the Xunta de Galicia have supported this manuscript through ENE2017-86425-C2-2-R, GRC ED431C 2020/10 and ED431E 2018/08 projects. Dr. María J. G. Guimarey acknowledges a postdoctoral fellowship from the Xunta de Galicia (Spain) and the financial support from IACOBUS programme.

References

[1] Y. Wu, W. Li, M. Zhang, X. Wang, Improvement of oxidative stability of trimethylolpropane trioleate lubricant, Thermochim. Acta 569 (2013) 112–118, https://doi.org/10.1016/j.tca.2013.05.033.
[2] S. Qiao, Y. Shi, X. Wang, Z. Lin, Y. Jiang, Synthesis of biolubricant trimethylolpropane trioleate and its lubricant base oil properties, Energy Fuels 31 (2017) 7185–7190, https://doi.org/10.1021/acs.energyfuels.7b00876.
[3] Y. Wu, W. Li, X. Wang, Synthesis and properties of trimethylolpropane trioleate as lubricating base oil, Lubr. Sci. 27 (2015) 369–379, https://doi.org/10.1002/ls.1287.
[4] Z.M. Zulfattah, N.W.M. Zulkifli, H.H. Masjuki, M.H. Harith, A.Z. Syahir, I. Norain, R. Jumaidin, M.N.A.M. Yusoff, A. Alwi, M. Jamshaid, A. Arslan, Effect of bio-based lubricant towards emissions and engine breakdown due to spark plug fouling in a two-stroke engine, J. Cleaner Prod. 221 (2019) 215–223, https://doi.org/10.1016/j.jclepro.2019.02.224.
[5] Y. He, T.J. Zolper, P. Liu, Y. Zhao, X. He, X. Shen, H. Sun, Q. Duan, Q. Wang, Elastohydrodynamic lubrication properties and friction behaviors of several

ester base stocks, Friction 3 (2015) 243–255, https://doi.org/10.1007/s40544-015-0090-6.
[6] J.M. Liñeira del Río, M.J.G. Guimarey, M.J.P. Comuñas, E.R. López, J.I. Prado, L. Lugo, J. Fernández, Tribological and thermophysical properties of environmentally-friendly lubricants based on trimethylolpropane trioleate with hexagonal boron nitride nanoparticles as an additive, Coatings 9 (2019) 509, https://doi.org/10.3390/coatings9080509.
[7] J.M. Liñeira del Río, M.J.G. Guimarey, M.J.P. Comuñas, E.R. López, A. Amigo, J. Fernández, Thermophysical and tribological properties of dispersions based on graphene and a trimethylolpropane trioleate oil, J. Mol. Liq. 268 (2018) 854–866, https://doi.org/10.1016/j.molliq.2018.07.107.
[8] E. Höglund, Influence of lubricant properties on elastohydrodynamic lubrication, Wear 232 (1999) 176–184, https://doi.org/10.1016/S0043-1648(99)00143-X.
[9] S. Bair, P. Michael, Modelling the pressure and temperature dependence of viscosity and volume for hydraulic fluids, Int. J. Fluid Power 11 (2010) 37–42, https://doi.org/10.1080/14399776.2010.10781005.
[10] A. Young, S. Bair, Experimental investigation of friction in entrapped elastohydrodynamic contacts, Tribol. Int. 43 (2010) 1615–1619, https://doi.org/10.1016/j.triboint.2010.03.007.
[11] S. Bair, High Pressure Rheology for Quantitative Elastohydrodynamics, Elsevier Science, Amsterdam, 2007.
[12] M. Hatami, M. Hasanpour, D. Jing, Recent developments of nanoparticles additives to the consumables liquids in internal combustion engines: Part II: Nano-lubricants, J. Mol. Liq. 319 (2020), https://doi.org/10.1016/j.molliq.2020.114156 114156.
[13] S.A.S. Amiril, E.A. Rahim, S. Syahrullail, A review on ionic liquids as sustainable lubricants in manufacturing and engineering: recent research, performance, and applications, J. Cleaner Prod. 168 (2017) 1571–1589, https://doi.org/10.1016/j.jclepro.2017.03.197.
[14] N.F. Azman, S. Samion, Dispersion stability and lubrication mechanism of nanolubricants: a review, Int. J. Precision Eng. Manuf.-Green Technol. 6 (2019) 393–414, https://doi.org/10.1007/s40684-019-00080-x.
[15] R. González, J.L. Viesca, A.H. Battez, M. Hadfield, A. Fernández-González, M. Bartolomé, Two phosphonium cation-based ionic liquids as lubricant additive to a polyalphaolefin base oil, J. Mol. Liq. 293 (2019), https://doi.org/10.1016/j.molliq.2019.111536 111536.
[16] L. Peña-Parás, D. Maldonado-Cortés, J. Taha-Tijerina, Eco-friendly nanoparticle additives for lubricants and their tribological characterization, in: L.M.T. Martínez, O.V. Kharissova, B.I. Kharisov, (Eds.), Handbook of Ecomaterials Springer Link, 2019, pp. 3247–3267.
[17] H. Spikes, Friction modifier additives, Tribol. Lett. 60 (2015) 1–26, https://doi.org/10.1007/s11249-015-0589-z.
[18] B.C. Stump, Y. Zhou, H. Luo, D.N. Leonard, M.B. Viola, J. Qu, New functionality of ionic liquids as lubricant additives: mitigating rolling contact fatigue, ACS Appl. Mater. Interfaces 11 (2019) 30484–30492, https://doi.org/10.1021/acsami.9b10001.
[19] L. Zhang, Y. He, L. Zhu, C. Yang, Q. Niu, C. An, In situ alkylated graphene as oil dispersible additive for friction and wear reduction, Ind. Eng. Chem. Res. 56 (2017) 9029–9034, https://doi.org/10.1021/acs.iecr.7b01338.
[20] L. Zhu, G. Zhao, X. Wang, Investigation on three oil-miscible ionic liquids as antiwear additives for polyol esters at elevated temperature, Tribol. Int. 109 (2017) 336–345, https://doi.org/10.1016/j.triboint.2016.10.032.
[21] J.M. Liñeira del Río, E.R. López, M. González Gómez, S. Yáñez Vilar, Y. Piñeiro, J. Rivas, D.E.P. Gonçalves, J.H.O. Seabra, J. Fernández, Tribological behavior of nanolubricants based on coated magnetic nanoparticles and trimethylolpropane trioleate base oil, Nanomaterials 10 (2020) 683, https://doi.org/10.3390/nano10040683.
[22] M.J.G. Guimarey, M.J.P. Comuñas, E.R. López, A. Amigo, J. Fernández, Thermophysical properties of polyalphaolefin oil modified with nanoadditives, J. Chem. Thermodyn. 131 (2019) 192–205, https://doi.org/10.1016/j.jct.2018.10.035.
[23] M.J.P. Comuñas, X. Paredes, F.M. Gaciño, J. Fernández, J.P. Bazile, C. Boned, J.L. Daridon, G. Galliero, J. Pauly, K.R. Harris, M.J. Assael, S.K. Mylona, Reference correlation of the viscosity of squalane from 273 to 373 K at 0.1 MPa, J. Phys. Chem. Ref. Data 42 (2013), https://doi.org/10.1063/1.4812573 033101.
[24] M.J.P. Comuñas, X. Paredes, F.M. Gaciño, J. Fernández, J.-P. Bazile, C. Boned, J.-L. Daridon, G. Galliero, J. Pauly, K.R. Harris, Viscosity measurements for squalane at high pressures to 350MPa from T=(293.15 to 363.15)K, J. Chem. Thermodyn. 69 (2014) 201–208, https://doi.org/10.1016/j.jct.2013.10.001.
[25] F.M. Gaciño, X. Paredes, M.J.P. Comuñas, J. Fernández, Effect of the pressure on the viscosities of ionic liquids: experimental values for 1-ethyl-3-methylimidazolium ethylsulfate and two bis(trifluoromethyl-sulfonyl)imide salts, J. Chem. Thermodyn. 54 (2012) 302–309, https://doi.org/10.1016/j.jct.2012.05.007.
[26] M. Dakkach, F.M. Gaciño, M.J.G. Guimarey, S.K. Mylona, X. Paredes, M.J.P. Comuñas, J. Fernández, M.J. Assael, Viscosity-pressure dependence for nanostructured ionic liquids. Experimental values for butyltrimethylammonium and 1-butyl-3-methylpyridinium bis(trifluoromethylsulfonyl)imide, J. Chem. Thermodyn. 121 (2018) 27–38, https://doi.org/10.1016/j.jct.2018.01.025.
[27] J.M. Liñeira del Río, M.J.G. Guimarey, M.J.P. Comuñas, J. Fernández, High pressure viscosity behaviour of tris(2-ethylhexyl) trimellitate up to 150 MPa, J. Chem. Thermodyn. 138 (2019) 159–166, https://doi.org/10.1016/j.jct.2019.06.016.
[28] M.J.P. Comuñas, J.P. Bazile, A. Baylaucq, C. Boned, Density of diethyl adipate using a new vibrating tube densimeter from (293.15 to 403.15) K and up to 140 MPa. Calibration and measurements, J. Chem. Eng. Data 53 (2008) 986–994, https://doi.org/10.1021/je700737c.
[29] F.M. Gaciño, T. Regueira, M.J.P. Comuñas, L. Lugo, J. Fernández, Density and isothermal compressibility for two trialkylimidazolium-based ionic liquids at temperatures from (278 to 398) K and up to 120 MPa, J. Chem. Thermodyn. 81 (2015) 124–130, https://doi.org/10.1016/j.jct.2014.09.014.
[30] T. Regueira, L. Lugo, J. Fernández, High pressure volumetric properties of 1-ethyl-3-methylimidazolium ethylsulfate and 1-(2-methoxyethyl)-1-methyl-pyrrolidinium bis(trifluoromethylsulfonyl)imide, J. Chem. Thermodyn. 48 (2012) 213–220, https://doi.org/10.1016/j.jct.2011.12.030.
[31] J.J. Segovia, O. Fandiño, E.R. López, L. Lugo, M.C. Martín, J. Fernández, Automated densimetric system: measurements and uncertainties for compressed fluids, J. Chem. Thermodyn. 41 (2009) 632–638, https://doi.org/10.1016/j.jct.2008.12.020.
[32] M. Hammami, R. Martins, M.S. Abbes, M. Haddar, J. Seabra, Axle gear oils: Tribological characterization under full film lubrication, Tribol. Int. 106 (2017) 109–122, https://doi.org/10.1016/j.triboint.2016.05.051.
[33] T.E. Tallian, On competing failure modes in rolling contact, ASLE Trans. 10 (1967) 418–439, https://doi.org/10.1080/05698196708972201.
[34] F.M. Gaciño, X. Paredes, M.J. Comuñas, J. Fernández, Pressure dependence on the viscosities of 1-butyl-2,3-dimethylimidazolium bis(trifluoromethylsulfonyl)imide and two tris(pentafluoroethyl) trifluorophosphate based ionic liquids: New measurements and modelling, J. Chem. Thermodyn. 62 (2013) 162–169, https://doi.org/10.1016/j.jct.2013.02.014.
[35] M.J.P. Comuñas, A. Baylaucq, C. Boned, J. Fernández, High-pressure measurements of the viscosity and density of two polyethers and two dialkyl carbonates, Int. J. Thermophys. 22 (2001) 749–768, https://doi.org/10.1023/a:1010770831215.
[36] K.V. Padmaja, B.V.S.K. Rao, R.K. Reddy, P.S. Bhaskar, A.K. Singh, R.B.N. Prasad, 10-Undecenoic acid-based polyol esters as potential lubricant base stocks, Ind. Crops Prod. 35 (2012) 237–240, https://doi.org/10.1016/j.indcrop.2011.07.005.
[37] A.S. Pensado, M.J.P. Comuñas, J. Fernández, Relationship between viscosity coefficients and volumetric properties: measurements and modeling for pentaerythritol esters, Ind. Eng. Chem. Res. 45 (2006) 9171–9183, https://doi.org/10.1021/ie0606035.
[38] A.S. Pensado, M.J.P. Comuñas, L. Lugo, J. Fernández, High-pressure characterization of dynamic viscosity and derived properties for squalane and two pentaerythritol ester lubricants: pentaerythritol tetra-2-ethylhexanoate and pentaerythritol tetrananonaoate, Ind. Eng. Chem. Res. 45 (2006) 2394–2404, https://doi.org/10.1021/ie051275w.
[39] X. Paredes, A.S. Pensado, M.J.P. Comuñas, J. Fernández, Experimental dynamic viscosities of dipentaerythritol Ester lubricants at high pressure, J. Chem. Eng. Data 55 (2010) 3216–3223, https://doi.org/10.1021/je100057b.
[40] K. Kamalakar, G.N.V.T.S. Manoj, R.B.N. Prasad, M.S.L. Karuna, Influence of structural modification on lubricant properties of sal fat-based lubricant base stocks, Ind. Crops Prod. 76 (2015) 456–466, https://doi.org/10.1016/j.indcrop.2015.07.050.
[41] H. van Leeuwen, The determination of the pressure—viscosity coefficient of a lubricant through an accurate film thickness formula and accurate film thickness measurements, Proc. Ins. Mech. Eng., Part J: J. Eng. Tribol. 223 (2009) 1143–1163. https://doi.org/10.1243/13506501jet504.
[42] H.A. Spikes, C.J. Hammond, The elastohydrodynamic film thicknesses of binary ester-ether mixtures, ASLE Trans. 24 (1981) 542–548, https://doi.org/10.1080/05698198108983054.
[43] P.W. Gold, A. Schmidt, H. Dicke, J. Loos, C. Assmann, Viscosity–pressure–temperature behaviour of mineral and synthetic oils, J. Synth. Lubr. 18 (2001) 51–79, https://doi.org/10.1002/jsl.3000180105.
[44] S. Bair, Y. Liu, Q.J. Wang, The pressure-viscosity coefficient for Newtonian EHL film thickness with general piezoviscous response, J. Tribol. 128 (2006) 624–631, https://doi.org/10.1115/1.2197846.
[45] X. Paredes, O. Fandiño, A.S. Pensado, M.J.P. Comuñas, J. Fernández, Pressure-viscosity coefficients for polyalkylene glycol oils and other ester or ionic lubricants, Tribol. Lett. 45 (2012) 89–100, https://doi.org/10.1007/s11249-011-9861-z.
[46] B.J. Hamrock, D. Dowson, Ball Bearing Lubrication: The Elastohydrodynamic of Elliptical Contacts, Wiley/Interscience, New York, 1981.
[47] I.M. Hutchings, Tribology: Friction and Wear of Engineering Materials, Edward Arnold, London, 1992.
[48] T.A. Stolarski, Tribology in Machine Design, Elsevier Science, United Kingdom, 2000.
[49] B.J. Hamrock, Fundamentals of Fluid Film Lubrication, McGraw-Hill, New York, 1994.
[50] G. Guangteng, H.A. Spikes, An experimental study of film thickness in the mixed lubrication regime, Tribol. Series 32 (1997) 159–166.
[51] H.A. Spikes, A.V. Olver, Basics of mixed lubrication, Lubr. Sci. 16 (2003) 1–28, https://doi.org/10.1002/ls.3010160102.
[52] D. Zhu, Q.J. Wang, On the λ ratio range of mixed lubrication, Proc. Inst. Mech. Eng., Part J: J. Eng. Tribol. 226 (2012) 1010–1022. https://doi.org/10.1177/1350650112461867.
[53] J. Guegan, A. Kadiric, A. Gabelli, H. Spikes, The relationship between friction and film thickness in EHD point contacts in the presence of longitudinal roughness, Tribol. Lett. 64 (2016) 33, https://doi.org/10.1007/s11249-016-0768-6.

[54] J.M. Liñeira del Río, E.R. López, J. Fernández, F. García, Tribological properties of dispersions based on reduced graphene oxide sheets and trimethylolpropane trioleate or PAO 40 oils, J. Mol. Liq. 274 (2019) 568–576, https://doi.org/10.1016/j.molliq.2018.10.107.